

# Geophysical Research Letters

## RESEARCH LETTER

10.1029/2018GL080494

### Key Points:

- The W. African monsoon, which expands northward in response to early Holocene orbital forcing, does not behave as an extension of the ITCZ
- The zonal-mean ITCZ either responds weakly or shifts southward in boreal summer, counter to the prevailing energetic framework
- Anomalous southward energy fluxes manifest as increased total gross moist stability rather than a northward ITCZ shift

### Supporting Information:

- Supporting Information S1

### Correspondence to:

J. E. Smyth,  
jsmyth@princeton.edu

### Citation:

Smyth, J. E., Hill, S. A., & Ming, Y. (2018). Simulated responses of the West African monsoon and zonal-mean tropical precipitation to early Holocene orbital forcing. *Geophysical Research Letters*, 45, 12,049–12,057. <https://doi.org/10.1029/2018GL080494>

Received 10 NOV 2017

Accepted 31 OCT 2018

Accepted article online 5 NOV 2018

Published online 9 NOV 2018

Corrected 3 DEC 2018

This article was corrected on 3 DEC 2018. See the end of the full text for details.

## Simulated Responses of the West African Monsoon and Zonal-Mean Tropical Precipitation to Early Holocene Orbital Forcing

Jane E. Smyth<sup>1</sup> , Spencer A. Hill<sup>2,3</sup> , and Yi Ming<sup>4</sup> 

<sup>1</sup>Program in Atmospheric and Oceanic Sciences, Princeton University, Princeton, NJ, USA, <sup>2</sup>Department of Atmospheric and Oceanic Sciences, University of California, Los Angeles, CA, USA, <sup>3</sup>Division of Geological and Planetary Sciences, California Institute of Technology, Pasadena, CA, USA, <sup>4</sup>Geophysical Fluid Dynamics Laboratory/NOAA, Princeton, NJ, United States

**Abstract** This study seeks to improve our mechanistic understanding of how the insolation changes associated with orbital forcing impact the West African monsoon and zonal-mean tropical precipitation. We impose early Holocene orbital parameters in simulations with the Geophysical Fluid Dynamics Laboratory AM2.1 atmospheric general circulation model, either with fixed sea surface temperatures, a 50-m thermodynamic slab ocean, or coupled to a dynamic ocean (CM2.1). In all cases, West African Monsoon rainfall expands northward, but the summer zonal-mean Intertropical Convergence Zone does not—there is drying near 10°N, and in the slab ocean experiment a southward shift of rainfall. This contradicts expectations from the conventional energetic framework for the Intertropical Convergence Zone location, given anomalous southward energy fluxes in the deep tropics. These anomalous energy fluxes are not accomplished by a stronger Hadley circulation; instead, they arise from an increase in total gross moist stability in the northern tropics.

**Plain Language Summary** Fossils, sediment records, and other evidence show that 10,000 years ago (10 ka), much of Northern Africa was substantially wetter. At the time, due to natural orbital variations, the Earth was closest to the sun during Northern Hemisphere (NH) summer, as opposed to NH winter today. This enhanced the equator-to-pole difference in incoming sunlight during NH summer. To better understand how this affected tropical rainfall, including the West African monsoon, we analyze atmospheric general circulation model simulations with either the modern or 10 ka orbital configuration. To isolate the role of sea surface temperature changes, one set of simulations fixes them at modern values, another represents the ocean as a static 50-m slab of water, and a third allows the ocean circulation to respond to the sunlight changes to respond to the sunlight changes. In all cases, the West African monsoon expands northward with the 10 ka orbit, consistent with fossil evidence. However, the NH summer tropical rainfall maximum moves southward, counter to the conventional understanding of how sunlight changes affect rainfall. Adjustments of the atmospheric circulation and its energy transport explain this result. This work improves our physical understanding of how the West African monsoon and the broader tropical precipitation respond to sunlight changes.

## 1. Introduction

Ample paleoclimate data indicate that 10,000 years ago (10 ka), near the beginning of the Holocene Epoch, much of Northern Africa was substantially wetter than today (e.g., Tierney et al., 2017, and references therein). This was the peak of the African Humid Period (15 to 5 ka), when increased humidity and vegetation characterized the modern Sahara (deMenocal, 2015). Past modeling studies imply that this largely resulted from an intensification and northward expansion of the West African monsoon (Joussame et al., 1999). At present, appreciable monsoon rainfall extends only as far north as the Sahel, the transitional region separating the Sahara Desert from the savannas to the south.

Precession is the primary orbital signal modulating Holocene insolation and rainfall over Africa relative to modern conditions (DeMenocal & Tierney, 2012). At 10 ka, perihelion occurred during Northern Hemisphere (NH) summer, as opposed to NH winter today. This intensified the NH seasonal cycle of insolation and weakened the SH seasonal cycle (Figure 1). A more oblique orbit at 10 ka relative to present was responsible for any

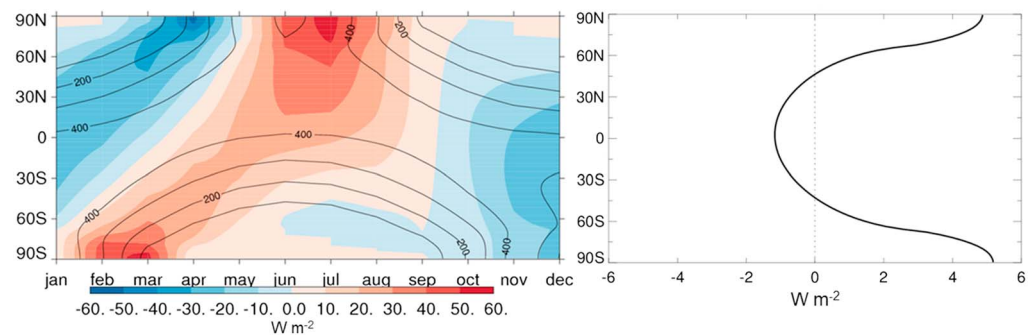


**Figure 1.** (left) Annual cycle of insolation (black contours) at present and (color shading) anomalies applied in the 10 ka simulations. (right) Annual mean 10 ka insolation anomalies.

annual mean insolation changes (Figure 1, right panel; Luan et al., 2012). Ice sheets and associated freshwater flux variations modulated the climate to a lesser extent (Marzin et al., 2013).

Based on previous studies linking anomalous cross-equatorial energy fluxes to the position of the zonal-mean Intertropical Convergence Zone (ITCZ), one would expect this orbitally driven insolation change to shift the ITCZ northward and strengthen its precipitation during NH summer (Bischoff et al., 2017; Schneider et al., 2014). However, though ITCZ responses to 10 ka-like precessional forcing are generally northward in coupled general circulation models (GCMs), they are often southward in slab ocean simulations, and in more idealized models the direction is sensitive to the land-ocean configuration (X. Liu et al., 2017; Merlis et al., 2013a, 2013c). X. Liu et al. (2017) describe that in 9 of 12 coupled models forced with mid-Holocene orbital parameters, southward atmospheric heat transport (AHT) manifests as a northward ITCZ shift. Three coupled models and a slab ocean model display counterintuitive southward ITCZ shifts, for which a physical mechanism was not determined. Further analysis is needed to assess the plausibility of this response and to explain the underlying processes.

It is also not clear how much an individual continental monsoon system such as the West African Monsoon is influenced by zonal-mean constraints (Roberts et al., 2017) or even by the behavior of the adjacent oceanic ITCZ. Monsoons can be thought of as driven by local meridional gradients of near-surface moist static energy (MSE; Emanuel, 1995; Hurley & Boos, 2013), which are likely altered by orbitally driven insolation changes independent of any zonal-mean constraints. Therefore, a particular focus is how the impacts of the imposed insolation gradient on dynamics and rainfall differ between the Sahel and the adjacent Atlantic Ocean.

## 2. Experimental Design

To clarify the influence of early Holocene orbital forcing on the West African monsoon and the zonal-mean climate, we present results from six simulations performed using the Geophysical Fluid Dynamics Laboratory AM2.1 atmospheric GCM (GFDL Global Atmospheric Model Development Team, 2004): with either modern or 10 ka orbital parameters, and with either prescribed SSTs, a 50-m slab ocean, or a coupled dynamic ocean model (CM2.1). The reference date for the model calendar is autumnal equinox (23 September). The prescribed sea surface temperatures (SSTs) are the climatological annual cycle from the Reynolds Optimum Interpolation data set (Reynolds et al., 2002) averaged over 1980–1999. The control AM2.1 simulation with a fixed annual cycle of SSTs captures the main features of the observed modern climatology over the Sahel (Hill et al., 2017). In the 50-m slab ocean configuration, SSTs vary with the atmospheric forcing, and a prescribed horizontal ocean heat flux is calibrated to reproduce present-day SSTs in the control simulation. In the coupled model, the boreal summer (June, July, August, or JJA) mixed layer depth across most of the North Atlantic ITCZ sector is 15–30 m (Figure S1). The model's land configuration does not feature dynamic vegetation, so associated albedo and soil moisture feedbacks which intensify the monsoon response are muted (e.g., Patricola & Cook, 2007). As such, all experiments underestimate the regional rainfall response compared to paleoclimate proxies (Tierney et al., 2011). We performed two additional simulations with only 10 ka obliquity or precession; the latter is dominant in the hydrological response (not shown).

The prescribed SST simulations span 17 years, with averages taken over the last 16 years. The slab ocean and coupled simulations span 40 and 200 years, respectively, with averages taken over the last 20 years. We

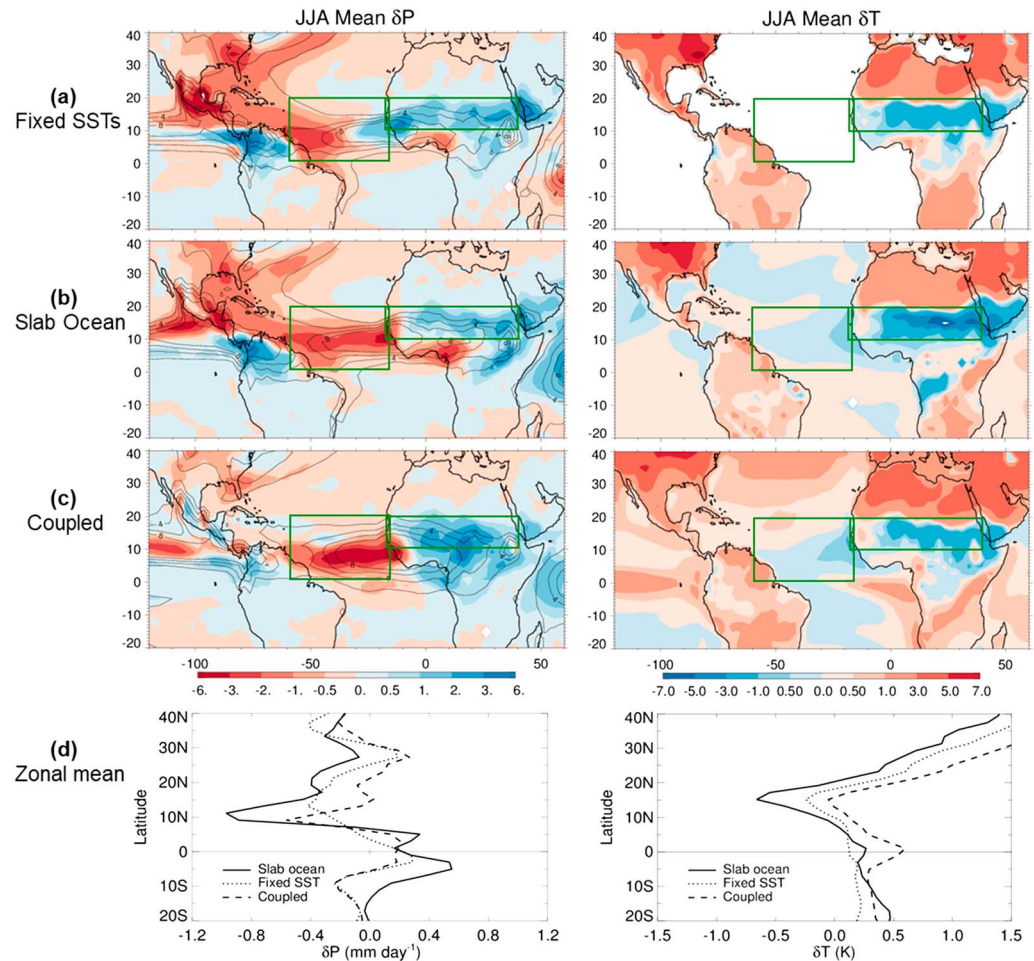


**Figure 2.** (left) JJA precipitation anomalies (10 ka-control, millimeter per day) in the three experiments: (a) fixed SSTs, (b) slab ocean, and (c) coupled dynamic ocean. (right) As above, but for temperature anomalies (K). In (d), anomalies are averaged over all longitudes. The green boxes delimit the North Atlantic Intertropical Convergence Zone and Sahel regions. The color bar intervals are pseudo-logarithmic. JJA = June, July, August; SST = sea surface temperature.

focus on JJA mean results, since this spans the period when the imposed insolation forcing is greatest in the tropics as well as the onset of the modern West African monsoon season. We also briefly discuss the annual mean response. Region-mean quantities were computed for the Sahel (land area within the domain 10 to 20°N, 18°W to 40°E) and for the Atlantic ITCZ (ocean area within the domain 0 to 20°N, 60 to 15°W). All vertically defined quantities use pressure-interpolated data, and these results do not differ importantly from those using data on model-native coordinates (not shown).

### 3. Results

#### 3.1. Atlantic ITCZ and Sahel Responses

In all simulations with 10 ka orbital parameters, the precipitation over the Sahel increases, in some places on the order of 100% (Figure 2). This northward expansion of the monsoon is in qualitative agreement with paleoclimate proxies. The monsoon strengthening is also evident in the wind field: each experiment exhibits anomalous onshore westerlies across the tropical Atlantic and southerly flow over the Sahel (Figure S2). Precipitation increases over West Africa by up to 2–3 mm/day in the prescribed SSTs and slab ocean experiments and up to 3–6 mm/day in the coupled model. Associated near-surface MSE maxima also shift northward (not shown), consistent with the argument that the precipitation and MSE maxima be nearly coincident (Prive & Plumb, 2007). In contrast, precipitation decreases over the Atlantic ITCZ sector, especially in the slab and dynamic ocean experiments (Figure 2). While the rainfall over coastal West Africa is continuous with the tropical Atlantic rainbelt in the climatology (e.g., Hastenrath, 1991), precipitation shifts in opposite directions

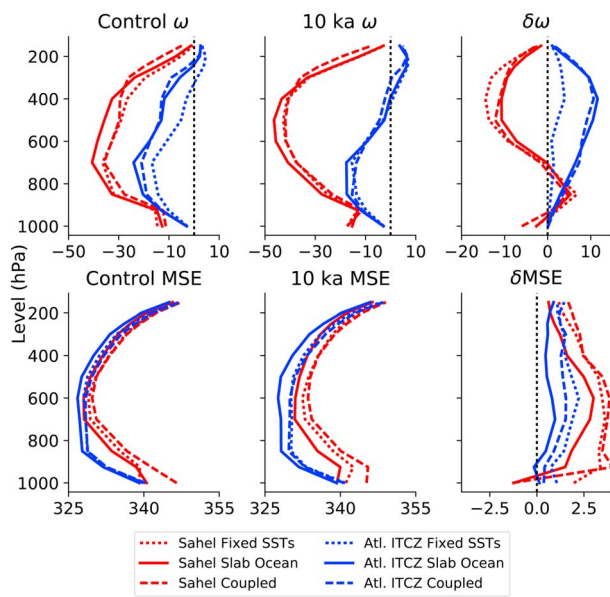


**Figure 3.** June, July, August vertical profiles of (top row)  $\omega$  (hPa/day) and (bottom row) MSE (K) in the control and 10 ka simulations, and their anomalies (10 ka-control). Results are averaged over the Sahel and North Atlantic ITCZ regions. MSE = moist static energy; SST = sea surface temperature; ITCZ = Intertropical Convergence Zone.

over the land and ocean with early Holocene orbital forcing. This zonal asymmetry is robust across model simulations of the early to mid-Holocene (Boos & Korty, 2016; Hsu et al., 2010; Z. Liu et al., 2004).

JJA surface temperatures decrease over the Sahel in the 10 ka simulations as precipitation increases, despite the locally increased insolation (Figure 2). In a supply-limited evaporative regime such as the semiarid Sahel, surface temperature and precipitation are generally tightly anticorrelated due to the impact of soil moisture on the partitioning of sensible and latent heat fluxes (e.g., Berg et al., 2015). The maximum cooling over the Sahel is between 1 and 3 K in the prescribed SST and coupled model experiments and up to 7 K in the slab ocean experiment (Figure 2). The positive insolation anomaly peaks in June, but due to the relatively deep, 50-m mixed layer in the slab ocean simulations, the Atlantic SST response lags the insolation by 2–3 months (Figure S3), such that JJA SSTs actually cool relative to the present day (Donohoe et al., 2014; Hsu et al., 2010). Section 4 further discusses the importance of the mixed layer depth. The precipitation response is similarly phase-lagged in the slab ocean experiment over the N. Atlantic ITCZ sector due to the strong control over tropical oceans of SSTs on rainfall (e.g., Neelin & Held, 1987). However, over the Sahel, the maximum precipitation anomaly occurs in JJA, in phase with the insolation anomaly, presumably due to the low land heat capacity.

The Sahel moistening is strongest in the coupled model experiment (Figure 2c), as in other studies noting enhanced land precipitation with the addition of ocean feedbacks (Z. Liu et al., 2004; Zhao et al., 2005). However,

the Atlantic dipole mode emphasized by Zhao et al. (2005), with warm Atlantic SST anomalies around 5°N and cold anomalies at 5°S, is not evident here. In both the slab and coupled ocean simulations, cold Atlantic SST anomalies off the West coast of Africa reduce the cross-equatorial SST gradient (Figure 2). We elaborate on the underlying surface energy budget response later in this section.

We now analyze terms of the MSE budget in the Sahel and Atlantic regions; see, for example, Hill et al. (2017) section 4(a) for a summary of the underlying theory. Figure 3 shows the vertical profiles of the regionally and seasonally averaged MSE and vertical velocity in pressure coordinates,  $\omega$ . Over the Sahel, anomalous ascent above approximately 700 hPa corresponds to a deepening of the circulation and greater export of MSE through vertical advection. The JJA subcloud (850 hPa) meridional MSE gradient decreases over the Sahel in the 10 ka simulations (not shown), which reduces horizontal MSE advection and necessitates more vertical MSE export. Consequently, the ascent profile deepens over the Sahel (Figure 3). There is a zero crossing in the  $\omega$  anomaly profile over the Sahel, and it occurs near the minimum ( $\sim 700$  hPa) in the MSE profile (Figure 3), likely because this is where the moist static stability ( $\partial h / \partial p$ ), where  $h$  is MSE, changes sign (Hill et al., 2017). The combined precipitation, circulation, and energetic responses over the Sahel with each lower boundary condition resemble those induced by uniform SST cooling in AM2.1 (Hill et al., 2017, c.f. their Figure 13).

Over the Atlantic sector, the vertical velocity weakens at all altitudes, with the strongest weakening at 400 hPa. This implies a shallowing of the circulation and thus a reduction in the vertical export of MSE. The lack of a dipole structure in  $\delta\omega$  over the Atlantic suggests distinct dynamical mechanisms in the two regions. The North Atlantic vertical velocity weakens much more in the slab ocean and coupled experiments than the fixed SSTs experiment, and is consistent with the similar SST cooling patterns in this sector (Figures 2b and 2c).

The anomalous descent over the Atlantic ITCZ sector motivated an energy budget analysis. The net energetic forcing term ( $F_{\text{net}}$ ) is equal to the total atmospheric energy flux divergence and comprises the sum of the top-of-atmosphere (TOA) radiative and surface radiative, sensible heat, and latent heat fluxes into the atmosphere (e.g., equation A4 of Hill et al., 2015). The region-mean  $F_{\text{net}}$  is negative in each experiment ( $-6.2$ ,  $-9.5$ ,  $-5.5$  W/m<sup>2</sup> in the fixed SST, slab ocean, and coupled experiments, respectively), consistent with weakened convection (c.f., Neelin & Held, 1987). An anomalous downward surface energy flux (driven primarily by short-wave and latent heat) outweighs the positive solar forcing at TOA. To first order, the reduced upward latent heat flux is caused by a weakening of the prevailing easterlies (Figure S2).



The distinct  $\omega$  responses over the North Atlantic and the Sahel in JJA imply an anomalous zonal circulation. The near-surface MSE increases more over the Sahel than over the tropical North Atlantic (Figure 3), and is associated with an enhanced monsoon circulation that shifts precipitation from ocean to land (Figure 2). A linear decomposition of the change in vertical MSE advection ( $(\omega \delta \frac{\partial h}{\partial p}) + (\delta \omega \frac{\partial h}{\partial p})$ ) shows that the response of  $\omega$  (second term) dominates the increase in energy export over the Sahel as well as the reduction over the Atlantic ITCZ sector in each experiment. The change in moist static stability (first term) in all cases modestly opposes the change in region-mean energy export driven by  $\delta \omega$ .

### 3.2. Zonal-Mean Response

Despite enhanced JJA NH insolation and associated southward anomalous energy fluxes (discussed below), the zonal-mean ITCZ shifts southward in JJA in the 10 ka simulations, though to a much lesser extent in the fixed SST case (Figure 2d). This runs counter to the prediction of energy flux equator (EFE) theory, the results of many coupled GCMs (X. Liu et al., 2017), and the locally northward rainfall migration over North Africa previously described. The zonal-mean response is dominated by the precipitation changes over the Pacific and Atlantic basins (Figure S4).

#### 3.2.1. Atmospheric Heat Transport

The AHT is the zonal and meridional integration of  $F_{\text{net}}$  minus atmospheric storage, where storage is the time-tendency of the column internal energy. The EFE, where tropical AHT equals zero, is located at  $\sim 12^\circ\text{N}$  in each control experiment (Figure 4a; Kang et al., 2008). The 10 ka forcing induces a northward EFE shift, or anomalous southward AHT at the control EFE latitude (Shekhar & Boos, 2016). In the coupled model, anomalous southward AHT extends from the North Pole to the SH subtropics, at the equator almost exactly compensating for a 0.13 PW wind-driven enhancement of northward cross-equatorial ocean heat transport. In the West Pacific and Indian Oceans, enhanced easterly winds along and north of the equator produce northward Ekman transport of warm water (not shown), as in X. Liu et al. (2017). The northward EFE shift in no case manifests as a northward ITCZ shift (Figure 2d).

#### 3.2.2. Hadley Circulation

Based on the zonal-mean meridional streamfunction (calculated c.f. equation A5 of Hill et al., 2015), the JJA southward energy flux is not primarily accomplished by a stronger Hadley cell mass flux (Figure 4b). Near  $10^\circ\text{N}$  where the zonal-mean drying is most pronounced, the zonal-mean circulation change is minimal ( $< \pm 8 \times 10^9$  kg/s) throughout the lower and midtroposphere in the fixed SSTs and coupled simulations (Figure 4b). The northern tropical circulation actually weakens in the slab ocean case with a maximum magnitude of  $35\text{--}40 \times 10^9$  kg/s (approximately 20%).

The Hadley circulation is governed by different physical regimes throughout the seasonal cycle, following variations in the local Rossby number ( $Ro$ ), defined as the negative ratio of the relative and planetary vorticities (e.g., Merlis et al., 2013a). In the slab ocean experiment, the JJA Hadley cell weakens only in the NH ascending branch, through a clockwise circulation that opposes the climatological overturning (Figure 4b). This is consistent with a regime in which the summer-hemisphere flank of the cross-equatorial Hadley cell conserves angular momentum ( $Ro \approx 1$ ; Merlis et al., 2013a). In this regime, the Hadley cell responds directly to the TOA energy balance (Held & Hou, 1980), while in the winter hemisphere it is restricted by extratropical eddies and nonlinear momentum fluxes (Merlis et al., 2013a; Walker & Schneider, 2006). Meridional SST gradients strongly constrain Hadley cell overturning strength (Singh et al., 2017), making its modest response in the fixed SST simulation unsurprising. In the slab ocean experiment, colder SST anomalies in the NH tropics slow the Hadley circulation. In the coupled model, the SST response varies between basins (not shown), resulting in a relatively small zonal-mean circulation change resembling the fixed SSTs experiment. Given that the Hadley circulation maintains its strength in the fixed SSTs and coupled model experiments, the zonal-mean precipitation changes are small. Though the JJA NH Hadley cell overturning strength does not change appreciably in these experiments, it achieves an additional southward AHT by other means, described next (Figure 4a).

#### 3.2.3. Total Gross Moist Stability

The total gross moist stability (GMS) is the ratio of AHT( $\phi$ ) to the mass transport  $\Psi(\phi)$  integrated to the pressure height of maximum intensity (Kang et al., 2009) and can be thought of as the efficiency of the export of energy by the total circulation, including the mean meridional circulation, stationary eddies, and transient eddies (Peters et al., 2008). In each 10 ka simulation the total GMS increases in the NH tropics (Figure 4c). In the slab ocean case, this more than compensates for the weakened overturning strength, thus generating southward energy flux anomalies. In the fixed SSTs and coupled model experiments, the increase in total GMS is large

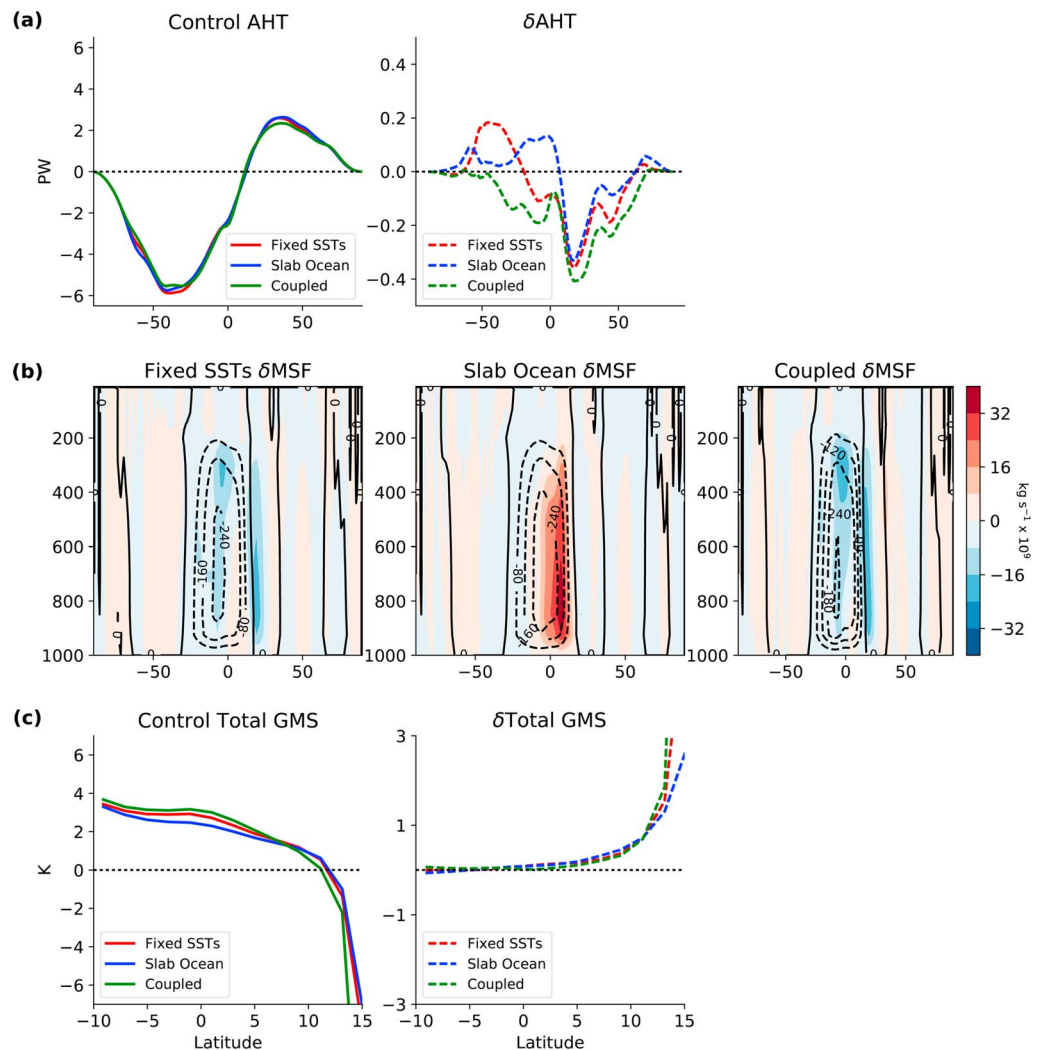


**Figure 4.** (a) AHT (left) in the control simulations and (right) the anomalies (10 ka-control). Positive values indicate northward heat transport. (b) Meridional MSF. Red indicates a clockwise circulation anomaly; black contours show control values. (c) Total GMS (left) in the control simulations and (right) the anomalies. AHT = atmospheric heat transport; SST = sea surface temperature; MSF = mass streamfunction; GMS = gross moist stability.

enough to balance the energy perturbation, since the Hadley circulation strength is less responsive to the forcing absent zonally coherent SST gradient anomalies.

The total GMS increase is reflected in elevated equivalent potential temperature aloft, which is likely linked to changes over land in the Northern tropics, including widespread warming and increased tropospheric relative humidity (not shown). Thus, even with modest surface MSE fluctuations over ocean, the zonal-mean energetic stratification of the atmosphere can dominate the zonal-mean climate response to forcing.

This response contradicts the simplistic picture in which tropical total GMS is set by the surface meridional MSE gradient. This understanding is based on two assumptions of tropical climate: that moist convection homogenizes MSE in the ascending branch of the Hadley cell, and that there is a weak temperature gradient aloft which sets the MSE in the upper Hadley cell branch to that of the ascending region (Held, 2001). In this framework, the total GMS is set by the surface meridional MSE contrast over the latitudinal extent of the Hadley cell, and would not be expected to change significantly in a climate with fixed SSTs in which the surface MSE response is confined to land.

### 3.3. Annual Mean Climate Response

The annual mean Hadley circulation anomaly in the slab ocean experiment qualitatively resembles the JJA response, with reduced ascent north of the equator (anomaly with maximum magnitude of 40% of the

climatological circulation strength; not shown). Since the branch of the cross-equatorial Hadley cell in the summer hemisphere is most responsive to radiative changes, the annual mean circulation change depends on the superposition of these solstitial changes throughout the year (Merlis et al., 2013a, 2013b). In the 10 ka simulations, the seasonal cycle strengthens in the NH and weakens in the SH compared to the present. Therefore, the summer ascending branch changes more in JJA than December, January, February, and the annual mean anomaly resembles the JJA anomaly. In the slab ocean experiment only, the zonal-mean cooling and drying in the northern tropics and warming and moistening in the southern tropics are also evident in the annual mean climate response (0.4–0.5 mm/day zonal-mean anomalies), consistent with Clement et al. (2004). The absence of a clear annual mean ITCZ shift in the fixed SSTs experiment suggests that the annual mean response is caused by a rectification of seasonally varying rainfall changes associated with Hadley cell dynamics, for which anomalous SST gradients are crucial.

The coupled model has a muted annual mean ITCZ response; precipitation increases by <0.25 mm/day near 15°N. The annual mean Hadley circulation response is correspondingly small, with only a minor (maximum magnitude of  $-12 \times 10^9$  kg/s) counterclockwise circulation anomaly above 400 hPa in the northern deep tropics. This modest northward ITCZ shift is consistent with the anomalous wind-driven annual mean northward cross-equatorial ocean heat transport (0.108 PW), though the two are not consistent in the JJA mean.

#### 4. Discussion

This study highlights that zonally symmetric orbital forcing can engender highly zonally asymmetric climate responses in the tropics. Regional differences in the temperature, MSE, and  $\omega$  perturbations give rise to differing precipitation responses over the Sahel and the adjacent North Atlantic ITCZ. In prescribed SST, slab ocean, and coupled model experiments, moistening over Africa in JJA is accompanied by a counterintuitive zonal-mean energetic and precipitation response. The JJA zonal-mean climate is dominated by the reduced precipitation over the Northern tropical oceans.

When SSTs are fixed, the circulation strength is constrained and the total GMS adjusts to achieve the cross-equatorial energy flux. When SSTs in a 50-m slab ocean interact with the forcing, they are anomalously cool in the NH tropics in JJA and result in a weaker Hadley circulation. The lag response of SSTs to insolation forcing amplifies the regional and zonal-mean JJA precipitation responses. In the coupled model simulation, the SST response varies between basins which results in a weak Hadley circulation response.

These results are consistent with a reduced July, August, September mean Hadley cell mass flux in the Merlis et al. (2013a) aquaplanet experiment with 10 ka precession. It is interesting that the zonal-mean circulation changes on an aquaplanet of 5-m depth are consistent with those in our study, which includes a substantially deeper mixed layer, full continental geometry, and a more comprehensive representation of atmospheric physics. The reduced mass flux in the Merlis et al. (2013a, 2013c) aquaplanet experiment was accompanied by an increase in NH tropical precipitation, which is not the case in our simulations. In the 5-m aquaplanet experiment, the surface heat capacity is small enough that the surface temperature changes are in phase with the insolation changes, driving increased surface specific humidity that leads to enhanced precipitation in the NH tropical summer, despite a weakening of the Hadley circulation. The influence of the slab ocean depth on the SST field and the associated precipitation response warrants further study (Donohoe et al., 2014). Also in contrast to our study, in simulations with a zonally symmetric subtropical continent, the summer Hadley cell mass flux increases and the ITCZ moves northward (Merlis et al., 2013b, 2013c).

The predictive model for the annual mean tropical precipitation response to orbital forcing proposed by Bischoff et al. (2017) does not capture the zonal-mean response to 10 ka orbital forcing reported here. That model predicts a strengthening of NH tropical precipitation, dominated by enhanced precipitation in NH summer, neither of which occurs in the fixed SSTs and slab ocean experiments. While annual mean precipitation slightly increases in the northern tropics of the coupled model experiment, it decreases in the NH summer. The assumption that the ITCZ position is proportional to the cross-equatorial atmospheric energy flux relies on a modest response of the total GMS, and does not account for the influence of zonal inhomogeneity.

X. Liu et al. (2017) assess 12 coupled model simulations with mid-Holocene orbital parameters and find that three models display southward ITCZ shifts, consistent with their ECHAM4.6 slab ocean simulation and the results reported here. They posit that this is due to radiative feedbacks or the inadequacy of the energetic

framework. Our analysis supports the latter, in that anomalous energy transports are not, as commonly assumed, generated purely through changes in overturning strength and associated ITCZ shifts.

It is difficult to validate any simulated zonal-mean precipitation response to orbital forcing based on available paleoclimate proxy records, due to ambiguity in whether these proxies are tracking seasonal or annual trends, combined with the scarcity of data over the ocean (Tigchelaar & Timmermann, 2016). Our results show that rainfall over the Sahel is not an extension of the ITCZ, so one cannot deduce the zonal-mean climate change from local proxies (Roberts et al., 2017). The coupled model results highlight that the annual climate response may not reflect the response in the season with the strongest insolation forcing.

In summary, an energetics-based analysis elucidates the regional and zonal-mean tropical precipitation responses to Holocene orbital forcing. Enhanced vertical export of MSE via deepening ascent intensifies rainfall over the Sahel and North Africa with 10 ka orbital parameters, even without SST changes. A southward JJA ITCZ shift (minimal in the fixed SSTs case) is accompanied in all experiments by an increase in the total GMS, and in the slab ocean experiment by a weakening of the Hadley circulation in the hemisphere with a brighter summer. The mechanisms we describe may provide a window into the varying hydrological responses of coupled models to Holocene orbital forcing.

### Acknowledgments

J.E.S. was partly supported by the NOAA Ernest F. Hollings Scholarship Program. S.A.H. is supported by an NSF AGS Postdoctoral Research Fellowship, NSF Award 1624740. Data used in this study can be retrieved from <http://osf.io/evfta>.

### References

- Berg, A., Lintner, B., Findell, K., Seneviratne, S., van den Hurk, B., Ducharne, A., et al. (2015). Interannual coupling between summertime surface temperature and precipitation over land: Processes and implications for climate change. *Journal of Climate*, 28, 1308–1328. <https://doi.org/10.1175/JCLI-D-14-00324.1>
- Bischoff, T., Schneider, T., & Meckler, A. N. (2017). A conceptual model for the response of tropical rainfall to orbital variations (Vol. 30, pp. 8375–8391). <https://doi.org/10.1175/JCLI-D-16-0691.1>
- Boos, W., & Korty, R. (2016). Regional energy budget control of the intertropical convergence zone and application to mid-Holocene rainfall. *Nature Geoscience*, 9, 892–897. <https://doi.org/10.1038/ngeo2833>
- Clement, A. C., Hall, A., & Broccoli, A. (2004). The importance of precessional signals in the tropical climate. *Climate Dynamics*, 22(4), 327–341. <https://doi.org/10.1007/s00382-003-0375-8>
- deMenocal, P. (2015). Paleoclimate: End of the African humid period. *Nature Geoscience*, 8, 86–87. <https://doi.org/10.1038/ngeo2355>
- DeMenocal, P., & Tierney, J. (2012). Green Sahara: African humid periods paced by Earth's orbital changes. *Nature Education Knowledge*, 3(10), 12.
- Donohoe, A., Frierson, D. M., & Battisti, D. S. (2014). The effect of ocean mixed layer depth on climate in slab ocean aquaplanet experiments. *Climate Dynamics*, 43(3–4), 1041–1055. <https://doi.org/10.1007/s00382-013-1843-4>
- Emanuel, K. A. (1995). On thermally direct circulations in moist atmospheres. *Journal of the Atmospheric Sciences*, 52(9), 1529–1534. [https://doi.org/10.1175/1520-0469\(1995\)052<1529:OTDCIM>2.0.CO;2](https://doi.org/10.1175/1520-0469(1995)052<1529:OTDCIM>2.0.CO;2)
- GFDL Global Atmospheric Model Development Team (2004). The new GFDL global atmosphere and land model AM2–LM2: Evaluation with prescribed SST simulations. *Journal of Climate*, 17(24), 4641–4673. <https://doi.org/10.1175/JCLI-3223.1>
- Hastenrath, S. (1991). *Climate dynamics of the tropics* (158 pp.). Dordrecht: Kluwer Academic Publishers. <https://doi.org/10.1007/978-94-011-3156-8>
- Held, I. (2001). The partitioning of the poleward energy transport between the tropical ocean and atmosphere. *Journal of the Atmospheric Sciences*, 58, 943–948. [https://doi.org/10.1175/1520-0469\(2001\)058<0943:TPOTPE>2.0.CO;2](https://doi.org/10.1175/1520-0469(2001)058<0943:TPOTPE>2.0.CO;2)
- Held, I. M., & Hou, A. Y. (1980). Nonlinear axially symmetric circulations in a nearly inviscid atmosphere. *Journal of the Atmospheric Sciences*, 37(3), 515–533. [https://doi.org/10.1175/1520-0469\(1980\)037<0515:NASCIA>2.0.CO;2](https://doi.org/10.1175/1520-0469(1980)037<0515:NASCIA>2.0.CO;2)
- Hill, S., Ming, Y., & Held, I. (2015). Mechanisms of forced tropical meridional energy flux change. *Journal of Climate*, 28, 1725–1742. <https://doi.org/10.1175/JCLI-D-14-00165.1>
- Hill, S. A., Ming, Y., Held, I. M., & Zhao, M. (2017). A moist static energy budget–based analysis of the Sahel rainfall response to uniform oceanic warming. *Journal of Climate*, 30(15), 5637–5660. <https://doi.org/10.1175/JCLI-D-16-0785.1>
- Hsu, Y. H., Chou, C., & Wei, K. Y. (2010). Land-ocean asymmetry of tropical precipitation changes in the mid-Holocene. *Journal of Climate*, 23, 4133–4151. <https://doi.org/10.1175/2010JCLI3392.1>
- Hurley, J., & Boos, W. (2013). Interannual variability of monsoon precipitation and local subcloud equivalent potential temperature. *Journal of Climate*, 26(23), 9507–9527. <https://doi.org/10.1175/JCLI-D-12-00229.1>
- Joussame, S., Taylor, K., Braconnot, P., Mitchell, J., Kutzbach, J., Harrison, S., et al. (1999). Monsoon changes for 6000 years ago: Results of 18 simulations from the Paleoclimate Modeling Intercomparison Project (PMIP). *Geophysical Research Letters*, 26, 859–862. <https://doi.org/10.1029/1999GL900126>
- Kang, S., Frierson, D., & Held, I. (2009). The tropical response to extratropical thermal forcing in an idealized GCM: The importance of radiative feedbacks and convective parameterization. *Journal of the Atmospheric Sciences*, 66, 2812–2827. <https://doi.org/10.1175/2009JAS2924.1>
- Kang, S., Held, I., Frierson, D., & Zhao, M. (2008). The response of the ITCZ to extratropical thermal forcing: Idealized slab-ocean experiments with a GCM. *Journal of Climate*, 21, 3521–3532. <https://doi.org/10.1175/2007JCLI2146.1>
- Liu, X., Battisti, D. S., & Donohoe, A. (2017). Tropical precipitation and cross-equatorial ocean heat transport during the mid-Holocene. *Journal of Climate*, 30(10), 3529–3547. <https://doi.org/10.1175/JCLI-D-16-0502.1>
- Liu, Z., Harrison, S. P., Kutzbach, J., & Otto-Bliesner, B. (2004). Global monsoons in the mid-Holocene and oceanic feedback. *Climate Dynamics*, 22(2–3), 157–182. <https://doi.org/10.1007/s00382-003-0372-y>
- Luan, Y., Braconnot, P., Yu, Y., Zheng, W., & Marti, O. (2012). Early and mid-Holocene climate in the tropical Pacific: Seasonal cycle and interannual variability induced by insolation changes. *Climate of the Past*, 8, 1093–1108. <https://doi.org/10.5194/cp-8-1093-2012>
- Marzin, T., Braconnot, P., & Kageyama, M. (2013). Relative impacts of insolation changes, meltwater fluxes and ice sheets on African and Asian monsoons during the Holocene. *Climate Dynamics*, 41, 2267–2286. <https://doi.org/10.1007/s00382-013-1948-9>



- Merlis, T., Schneider, T., Bordoni, S., & Eisenman, I. (2013a). Hadley circulation response to orbital precession. Part I: Aquaplanets. *Journal of Climate*, 26, 740–753. <https://doi.org/10.1175/JCLI-D-11-00716.1>
- Merlis, T., Schneider, T., Bordoni, S., & Eisenman, I. (2013b). Hadley circulation response to orbital precession. Part II: Subtropical continent. *Journal of Climate*, 26, 754–771. <https://doi.org/10.1175/JCLI-D-12-00149.1>
- Merlis, T., Schneider, T., Bordoni, S., & Eisenman, I. (2013c). The tropical precipitation response to orbital precession. *Journal of Climate*, 26, 2010–2021. <https://doi.org/10.1175/JCLI-D-12-00186.1>
- Neelin, D., & Held, I. (1987). Modeling tropical convergence based on the moist static energy budget. *Monthly Weather Review*, 115, 3–12. [https://doi.org/10.1175/1520-0493\(1987\)115<0003:MTCBOT>2.0.CO;2](https://doi.org/10.1175/1520-0493(1987)115<0003:MTCBOT>2.0.CO;2)
- Patricola, C. M., & Cook, K. H. (2007). Dynamics of the West African monsoon under mid-Holocene precessional forcing: Regional climate model simulations. *Journal of Climate*, 20, 694–716. <https://doi.org/10.1175/JCLI4013.1>
- Peters, M., Kuang, Z., & Walker, C. (2008). Analysis of atmospheric energy transport in ERA-40 and implications for simple models of the mean tropical circulation. *Journal of Climate*, 21, 5229–5241. <https://doi.org/10.1175/2008JCLI2073.1>
- Prive, N. C., & Plumb, A. R. (2007). Monsoon dynamics with interactive forcing. Part I: Axisymmetric studies. *Journal of the Atmospheric Sciences*, 64, 1417. <https://doi.org/10.1175/JAS3916.1>
- Reynolds, R. W., Rayner, N. A., Smith, T. M., Stokes, D. C., & Wang, W. (2002). An improved in situ and satellite SST analysis for climate. *Journal of Climate*, 15(13), 1609–1625. [https://doi.org/10.1175/1520-0442\(2002\)015<1609:AIISAS>2.0.CO;2](https://doi.org/10.1175/1520-0442(2002)015<1609:AIISAS>2.0.CO;2)
- Roberts, W. H. G., Valdes, P. J., & Singarayer, J. S. (2017). Can energy fluxes be used to interpret glacial/interglacial precipitation changes in the tropics? *Geophysical Research Letters*, 44, 6373–6382. <https://doi.org/10.1002/2017GL073103>
- Schneider, T., Bischoff, T., & Huang, G. (2014). Migrations and dynamics of the intertropical convergence zone. *Nature Review*, 513, 45–53. <https://doi.org/10.1038/nature13636>
- Shekhar, R., & Boos, W. (2016). Improving energy-based estimates of monsoon location in the presence of proximal deserts. *Journal of Climate*, 29, 4741–4761. <https://doi.org/10.1175/JCLI-D-15-0747.1>
- Singh, M. S., Kuang, Z., & Tian, Y. (2017). Eddy influences on the strength of the hadley circulation: Dynamic and thermodynamic perspectives. *Journal of the Atmospheric Sciences*, 74(2), 467–486. <https://doi.org/10.1175/JAS-D-16-0238.1>
- Tierney, J., Lewis, S., Cook, B., LeGrande, A., & Schmidt, G. (2011). Model, proxy and isotopic perspectives on the East African humid period. *Earth and Planetary Science Letters*, 307, 103–112. <https://doi.org/10.1016/j.epsl.2011.04.038>
- Tierney, J., Pausata, F., & deMenocal, P. (2017). Rainfall regimes of the Green Sahara. *Science Advances*, 3(1), E1601503. <https://doi.org/10.1126/sciadv.1601503>
- Tigchelaar, M., & Timmermann, A. (2016). Mechanisms rectifying the annual mean response of tropical Atlantic rainfall to precessional forcing. *Climate Dynamics*, 47(1–2), 271–293. <https://doi.org/10.1007/s00382-015-2835-3>
- Walker, C. C., & Schneider, T. (2006). Eddy influences on hadley circulations: Simulations with an idealized GCM. *Journal of the Atmospheric Sciences*, 63(12), 3333–3350. <https://doi.org/10.1175/JAS3821.1>
- Zhao, Y., Braconnot, P., Marti, O., Harrison, S. P., Hewitt, C., Kitoh, A., et al. (2005). A multi-model analysis of the role of the ocean on the African and Indian monsoon during the mid-Holocene. *Climate Dynamics*, 25(7–8), 777–800. <https://doi.org/10.1007/s00382-005-0075-7>

## Erratum

In the originally published version of this article, a typographical error was introduced into the Plain Language Summary. The fifth sentence should have correctly read “To isolate the role of sea surface temperature changes, one set of simulations fixes them at modern values, another represents the ocean as a static 50-m slab of water, and a third allows the ocean circulation to respond to the sunlight changes to respond to the sunlight changes.” The error has since been corrected, and the present version may be considered the authoritative version of record.